

## NONLINEAR DYNAMOS: A COMPLEX GENERALIZATION OF THE LORENZ EQUATIONS

C.A. JONES

*School of Mathematics, University of Newcastle-upon-Tyne, England NE1 7RU*

N.O. WEISS and F. CATTANEO

*Department of Applied Mathematics and Theoretical Physics, University of Cambridge, England CB3 9EW*

Received 29 August 1983

Revised 22 May 1984

Plane nonlinear dynamo waves can be described by a sixth order system of nonlinear ordinary differential equations which is a complex generalization of the Lorenz system. In the regime of interest for modelling magnetic activity in stars there is a sequence of bifurcations, ending in chaos, as a stability parameter  $D$  (the dynamo number) is increased. We show that solutions undergo three successive Hopf bifurcations, followed by a transition to chaos. The system possesses a symmetry and can therefore be reduced to a fifth order system, with trajectories that lie on a 2-torus after the third bifurcation. As  $D$  is then increased, frequency locking occurs, followed by a sequence of period-doubling bifurcations that leads to chaos. This behaviour is probably caused by the Shil'nikov mechanism, with a (conjectured) homoclinic orbit when  $D$  is infinite.

### 1. Introduction

Stars like the sun exhibit irregular cycles of magnetic activity and the 11-year sunspot cycle provides a good example of aperiodic oscillations. The corresponding magnetic cycle, with an average period of 22 years, is caused by dynamo action within the sun. The generation of large scale magnetic fields can be modelled by equations that yield plane waves in a cartesian system [1]. These linear equations can be extended by adding various nonlinear effects in order to model dynamo waves of finite amplitude. Of the various nonlinear systems discussed in [2] and [3], the most interesting is the sixth order system

$$\begin{aligned}\dot{A} &= 2DB - A, \\ \dot{B} &= iA - \frac{1}{2}iA^*\omega - B, \\ \dot{\omega} &= -iAB - \nu\omega,\end{aligned}\tag{1.1}$$

where the variables  $A(t)$ ,  $B(t)$ ,  $\omega(t)$  are complex, while  $\nu$  and  $D$  are real, positive parameters [2].

Here  $A$  and  $B$  represent poloidal and toroidal magnetic fields, while  $\omega$  describes fluctuations in differential rotation. For  $\nu < 1$  there is a sequence of bifurcations as  $D$  is increased, leading to chaotic behaviour with episodes of reduced activity that bears a strong qualitative resemblance to the pattern of variation of magnetic activity in the sun. The astrophysical implications of these results have been discussed elsewhere [2, 3]. It is also important to establish how the transition from periodic to chaotic behaviour occurs. In this paper we show that there are three successive Hopf bifurcations, resulting in quasiperiodic motion, followed by frequency locking and a cascade of period-doubling bifurcations that leads to chaos. We suggest that this behaviour is associated with the existence of an unstable homoclinic orbit when  $D$  is infinite. Provided that such an orbit exists, chaos will occur, since the eigenvalues at the origin in phase space satisfy Shil'nikov's condition [4]. We therefore argue that the mechanism is robust and not just a feature of the simple system (1.1).

Eqs. (1.1) are a special case of the system

$$\begin{aligned} \dot{A} &= \sigma^{1/2}(\sigma + 1)DB - \sigma A, \\ \dot{B} &= iA - \frac{1}{2}iA^*\omega - B, \\ \dot{\omega} &= -iAB - \nu\omega, \end{aligned} \quad (1.2)$$

with  $\sigma = 1$ . If we set  $A = \sqrt{2}x$ ,  $B = \sqrt{2}iy/R$ ,  $\omega = 2z/R$ , where  $R = i\sigma^{-1/2}(\sigma + 1)D$ , then (1.2) reduces to

$$\begin{aligned} \dot{x} &= \sigma(y - x), \\ \dot{y} &= Rx - x^*z - y, \\ \dot{z} &= xy - \nu z, \end{aligned} \quad (1.3)$$

which is a complex generalization of the real, third order Lorenz system [5, 6]. In what follows we shall therefore consider the more general system (1.2), with  $\sigma$  real and positive, though detailed numerical results will be confined to the case  $\sigma = 1$ . The physical derivation indicates that the constants  $\nu$  and  $\sigma$  are of order unity, while  $D$  is related to the Rayleigh number  $R$  in the Lorenz system. We shall therefore consider the bifurcations that occur as  $D$  is increased from zero, for fixed values of  $\nu$  and  $\sigma$ .

The sixth order system (1.3) has a somewhat richer structure than fifth order complex generalizations of the Lorenz system (1.4). For instance, another model of nonlinear dynamo waves yields the system

$$\begin{aligned} \dot{x} &= \sigma(y - x), \\ \dot{y} &= Rx - xz - y, \\ \dot{z} &= \frac{1}{2}(x^*y - xy^*) - \nu z, \end{aligned} \quad (1.4)$$

where  $z$  is purely imaginary [2, 3]. (Jones [7] has discussed the case  $\nu = 0$  for a closely related system.) The system (1.4) is not essentially different from the complex Lorenz equations studied by Fowler et al. [8] and Booty et al. [9]. (In their system  $z$  is real and the nonlinear source term in the third equation is  $\text{Re}(x^*y)$  rather than  $\text{Im}(x^*y)$ .) Both systems possess nonlinear periodic solutions for  $D > 1$  which can be expressed

analytically in terms of trigonometric functions. For  $\sigma \leq 1$  there are stable limit cycles for all  $D \geq 1$ ; however, if  $\sigma$  is sufficiently large the periodic solutions can become unstable in the manner discussed by Fowler et al. [8].

The outline of this paper is as follows. In the next section we present some numerical results, illustrating the transition from ordered to chaotic behaviour in solutions of (1.1), in order to motivate subsequent discussion. Then, in section 3, we show that the sixth order system (1.2) possesses a symmetry that allows it to be reduced to a fifth order system, and investigate nonlinear solutions after the first bifurcation at  $D = 1$  (corresponding to limit cycles and singular points for the sixth and fifth order systems respectively). The stability of these solutions is analysed in section 4; for a suitable choice of parameters there is a Hopf bifurcation leading to motion on a 2-torus and a limit cycle respectively. At the next bifurcation, discussed in section 5, 3-tori and 2-tori appear respectively. For the case  $\sigma = 1$ ,  $\nu = 0.5$  we describe the transition, through frequency locking on the 2-torus followed by a cascade of period-doubling bifurcations, to a chaotic regime which apparently persists for all finite values of  $D$ . Finally, in the conclusion, we conjecture that the appearance of chaos is associated with a homoclinic bifurcation when  $D$  is infinite, and that the pattern of bifurcations found for (1.2) is therefore likely to be shared by other, more complicated systems.

## 2. Bifurcations in the sixth order system

We first establish some general properties of the system (1.2). The equations possess an obvious symmetry, for they are invariant under the transformation  $(A, B, \omega, D) \rightarrow (A^*, -B^*, \omega^*, -D)$ . Although negative values of  $D$  are physically meaningless, any solution for negative  $D$  corresponds to one for positive  $D$ . Thus it suffices to consider behaviour for  $D \geq 0$ . For all  $D$  there exists a trivial solution  $A = B = \omega = 0$ . To study

the stability of this solution to small disturbances, we neglect the quadratic terms in equations (1.2) to obtain

$$\frac{d}{dt} \begin{pmatrix} A \\ B \\ \omega \end{pmatrix} = \begin{pmatrix} -\sigma & \sigma^{1/2}(\sigma+1)D & 0 \\ i & -1 & 0 \\ 0 & 0 & \nu \end{pmatrix} \begin{pmatrix} A \\ B \\ \omega \end{pmatrix}, \quad (2.1)$$

which has eigenvalues

$$-\nu, \frac{1}{2} \left[ -(\sigma+1) \pm \left\{ (\sigma-1)^2 + 4i\sigma^{1/2}(\sigma+1)D \right\}^{1/2} \right].$$

The first eigenvalue is always stable and instability occurs only with the positive square root. It can readily be shown that the trivial solution is stable to small perturbations for  $D \leq 1$  and unstable for  $D > 1$ . There is a Hopf bifurcation at  $D = 1$  and the neutrally stable mode has a frequency  $\sigma^{1/2}$ . We call this bifurcation (A).

The bifurcation may be subcritical, as we shall see in section 3. To obtain a global stability result we consider the Lyapunov function

$$L \equiv \sigma^{-1}|A|^2 + 2|B|^2 + |\omega|^2. \quad (2.2)$$

Then, from (1.2),

$$\begin{aligned} \frac{dL}{dt} = & -|2B - \left\{ \frac{1}{2}\sigma^{-1/2}(\sigma+1)D + i \right\} A|^2 \\ & - 2\nu|\omega|^2 + \left\{ (\sigma+1)^2 D^2 / 4\sigma - 1 \right\} |A|^2, \end{aligned} \quad (2.3)$$

so that  $L$  is always decreasing provided  $D < 2\sigma^{1/2}/(\sigma+1)$ . Hence the trivial solution is globally attracting for

$$0 \leq D < 2\sigma^{1/2}/(\sigma+1) \leq 1. \quad (2.4)$$

When  $\sigma = 1$  the local and global stability criteria coincide but in general the latter is weaker, as one would expect.

A branch of oscillatory solutions bifurcates from  $D = 1$ . As was found in [7], [8] and [9], solutions

on this branch can be expressed analytically in terms of trigonometric functions. Substituting

$$A = a e^{i p t}, \quad B = b e^{i(p t + \phi)}, \quad \omega = \Omega a^2 e^{2 i p t} \quad (2.5)$$

into (1.2), we find that

$$\begin{aligned} b &= \frac{(\sigma^2 + p^2)^{1/2} a}{\sigma^{1/2}(\sigma+1)D}, \\ \Omega &= -\frac{i(\sigma+i p)(\nu-2i p)}{\sigma^{1/2}(\sigma+1)(\nu^2+4p^2)}, \end{aligned} \quad (2.6)$$

$$\tan \phi = p,$$

where  $p$  satisfies the cubic equation

$$\begin{aligned} (2+\nu)p^3 - 2\sigma^{1/2}(\sigma+1)Dp^2 \\ + (\nu+2)\sigma^2 p - \nu\sigma^{3/2}(\sigma+1)D = 0 \end{aligned} \quad (2.7)$$

and

$$\begin{aligned} a^2 = (2/\sigma) [(\nu+2\sigma+2)p^2 \\ - 2\sigma^{1/2}(\sigma+1)Dp - \nu\sigma] \geq 0. \end{aligned} \quad (2.8)$$

As expected, (2.7) has a root  $p = \sigma^{1/2}$  when  $D = 1$ , with a corresponding value of  $a = 0$  from (2.8).

When  $\sigma = 1$  the periodic solution (2.5) eventually becomes unstable for all  $\nu < 1$ . In the remainder of this section we describe solutions obtained for  $\nu = 0.5, \sigma = 1$ . Then there is a stable limit cycle for  $1 < D < 2.07$ . At  $D \approx 2.07$  this solution undergoes a Hopf bifurcation: in the return map a pair of complex conjugate eigenvalues (Floquet multipliers) crosses the unit circle. Beyond this bifurcation there are doubly periodic solutions of (1.1) and stable trajectories lie on a 2-torus enclosing the unstable periodic solution (2.5). Fig. 1a shows a projection of this 2-torus onto the  $B_r \omega_r$  plane for  $D = 3$ . The Poincaré return map in the same plane, for  $A_r = 0$ , demonstrates the existence of a torus. (Here  $A_r, B_r, \omega_r$  are the real parts of  $A, B$  and  $\omega$  respectively.) At  $D \approx 3.47$  there is a third Hopf bifurcation, leading

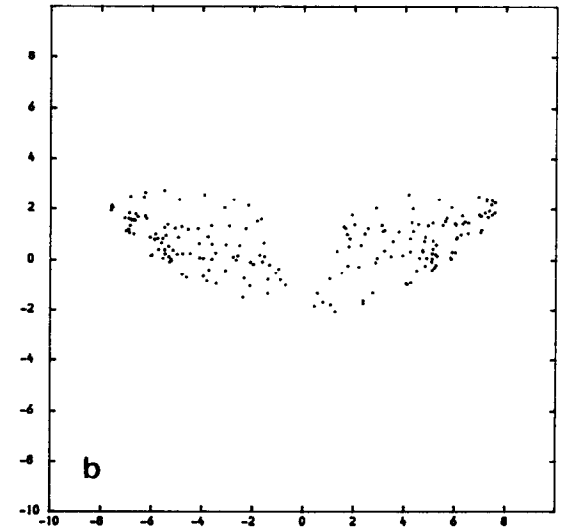
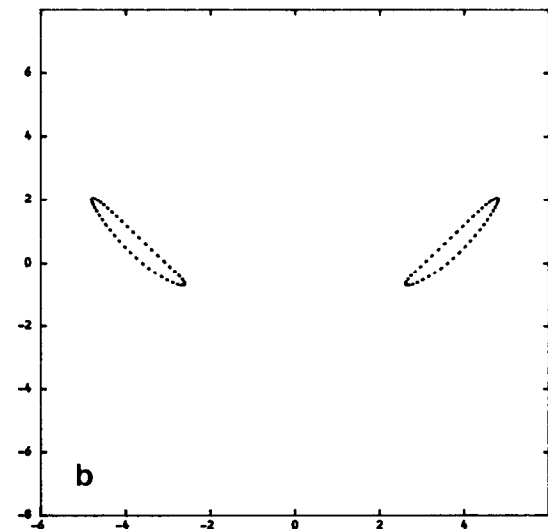
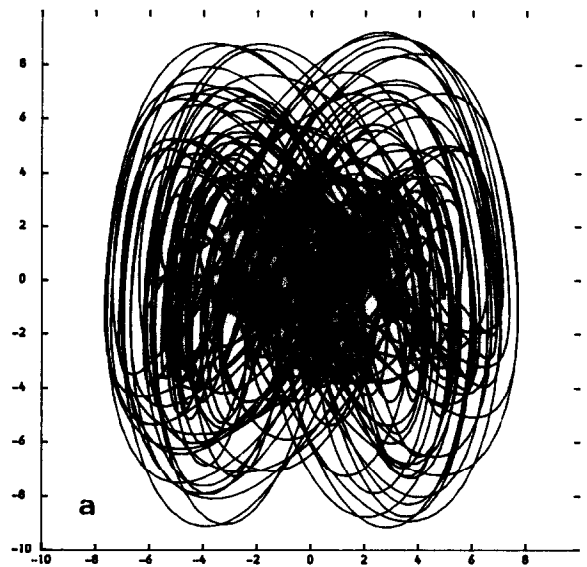
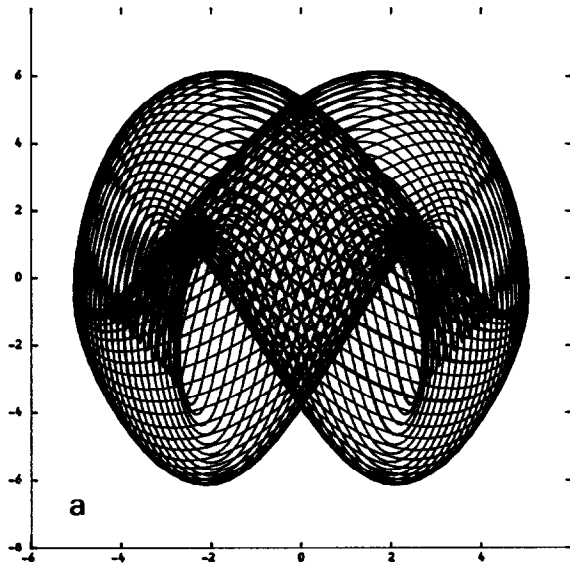


Fig. 1. a) A projection of a trajectory for the sixth order system (1.1) with  $\sigma = 1$ ,  $\nu = \frac{1}{2}$  and  $D = 3.0$ . The projection is onto the  $B_r\omega_r$ -plane. b) The Poincaré map for the same plane as in a), taking the section  $A_r = 0$ .

Fig. 2. a) As for 1a, but with  $D = 3.6$ ; b) As for 1b, but with  $D = 3.6$ .

to triply periodic motion on a 3-torus. Fig. 2 shows a projection of this 3-torus onto the  $B_r\omega_r$  plane, with the corresponding return map. The latter shows that trajectories no longer lie on a 2-torus. Finally, by  $D = 4.0$ , there is a transition to chaotic behaviour, as shown for  $D = 8.0$  in fig. 3.

Time series plots, showing  $B_r(t)$  are illustrated in [3]. They show aperiodic modulation of the cyclic pattern, with intervals while  $|B|$  remains small and trajectories hover near the origin in phase space. In the remainder of this paper we investigate the bifurcations that lead to such behaviour.

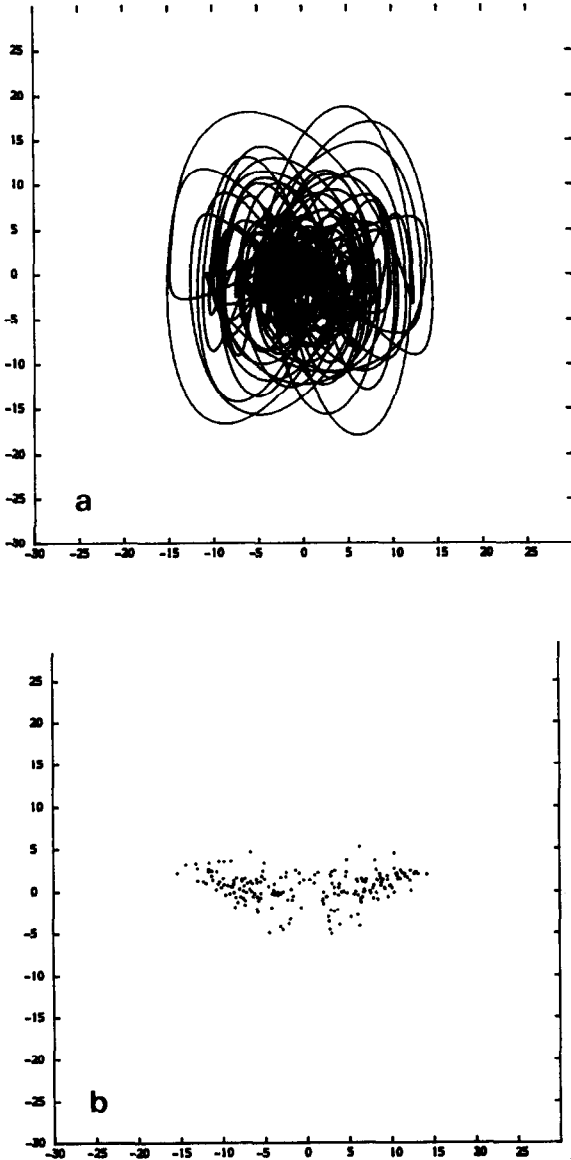


Fig. 3. a) As for 1a, but with  $D = 8.0$ ; b) As for 1b, but with  $D = 8.0$ .

### 3. Reduction to a fifth order system

The sixth order system (1.2) possesses a further symmetry. We may generalize (2.5) by introducing polar coordinates and writing

$$A = 2r e^{i\theta} = 2\rho^{1/2} e^{i\theta}, \tag{3.1}$$

so that  $\rho = r^2$ , and setting

$$B = \left(\frac{\rho}{\sigma}\right)^{1/2} \frac{2x}{(\sigma + 1)D} e^{i\theta}, \tag{3.2}$$

$$\omega = \frac{2y}{D\sigma^{1/2}(\sigma + 1)} e^{2i\theta}.$$

Substituting into (1.2) from (3.1) and (3.2), we find that  $\theta$  does not appear explicitly in the new equations, which reduce to the fifth order system

$$\begin{aligned} \dot{\rho} &= \rho(x + x^*) - 2\sigma\rho, \\ \dot{x} &= i\sigma^{1/2}(\sigma + 1)D - iy - x^2 + (\sigma - 1)x, \\ \dot{y} &= -2i\rho x - y(x - x^*) + \nu y, \end{aligned} \tag{3.3}$$

where  $x$  and  $y$  are complex but  $\rho$  is real. The ignorable variable  $\theta$ , which is just a phase factor in the original system, can be obtained from

$$\dot{\theta} = -\frac{1}{2}i(x - x^*). \tag{3.4}$$

The limit cycle shed at bifurcation (A) is obtained from a (nontrivial) steady solution of (3.3), with  $x = \sigma + ip$ , where  $p$  satisfies (2.7) and  $\rho$  can be obtained from (2.8). For the solution to be acceptable it is, of course, necessary that  $\rho = \frac{1}{4}a^2 \geq 0$ . Perturbing  $p$  and  $D$  and using (2.7) and (2.8), we discover that the Hopf bifurcation is supercritical if

$$\sigma(2 - \nu) < 2 + 3\nu \tag{3.5}$$

and subcritical if  $\sigma$  is greater than this value. We note that (2.4) implies that in subcritical cases, we can never have a solution for  $D < 2\sigma^{1/2}/(\sigma + 1)$ , which puts a limit on the possible depth of subcriticality. When the bifurcation is subcritical there are two steady solutions of (3.3) for  $D$  just below 1. The solution with a lower value of  $\rho$  is always unstable. But the solutions with a larger value of  $\rho$  can, in some circumstances, be stable. In supercritical cases, there is always one steady solution of (3.3) for  $D > 1$ , and for  $\sigma$  sufficiently large there can be up to 3 solutions.

Because the nonlinear solution after bifurcation (A) has such a simple form, it is possible to discuss its stability analytically. We introduce the 5-vector  $\mathbf{u} = (\rho, x_r, x_i, y_r, y_i)$ , where  $x_r, x_i, y_r$  and  $y_i$  are the real and imaginary parts of  $x$  and  $y$ . Then system (3.3) can be written

$$\frac{d u_i}{d t} = c_i + a_{ij} u_j + b_{ijk} u_j u_k, \tag{3.6}$$

where the coefficients  $a_{ij}$  and  $b_{ijk}$  depend only on  $\sigma$  and  $\nu$ . Steady solutions  $\mathbf{u}^0$  satisfy (3.6) with  $d/dt \equiv 0$ . To examine stability, we write

$$\mathbf{u} = \mathbf{u}^0 + \epsilon \mathbf{u}^1 e^{qt} + \mathcal{O}(\epsilon^2), \tag{3.7}$$

so we must solve the eigenvalue problem

$$q u_i^1 = a_{ij} u_j^1 + b_{ijk} (u_j^0 u_k^1 + u_j^1 u_k^0); \tag{3.8}$$

$q$  is then determined by the quintic equation

$$\begin{aligned} q^5 + 2(\sigma + \nu + 1)q^4 \\ + [6p^2 + 4\rho + (\sigma + 2)^2 + 4\sigma\nu + (\nu + 2)^2 - 7]q^3 \\ + 2c_1 q^2 + c_2 q \\ + 4\rho [(\nu + 2)(3p^2 + \sigma) - 4pD\sigma^{1/2}(\sigma + 1)] = 0, \end{aligned} \tag{3.9}$$

where

$$\begin{aligned} c_1 = p^2(3\sigma + \nu + 3) + 2\rho(4\sigma + \nu + 1) \\ + (1 + \sigma\nu)(\sigma + \nu) + \sigma^2 + 5\sigma\nu + \nu^2, \\ c_2 = 24p^4 + [(\nu - 2)^2 + (2\sigma - \nu)^2 - 4\rho] p^2 \\ + \nu^2(\sigma^2 + 1) + 4\sigma\nu(\sigma + \nu + 1) \\ + \rho[12\sigma(\nu + 1) + 4(\nu + \rho)]. \end{aligned} \tag{3.10}$$

Some insight can be gained into the nature of this quintic by considering its properties at large  $D$ . Then

$$\begin{aligned} p \sim \frac{D\sigma^{1/2}}{(\sigma + 1)} \left\{ \frac{2(\sigma + 1)^2}{(\nu + 2)} + \frac{(\nu - 2\sigma)(\nu + 2)}{4D^2} \right\} \\ + \mathcal{O}(D^{-3}), \quad \rho \sim \mathcal{O}(D^2) \end{aligned} \tag{3.11}$$

and four roots have  $q \sim \mathcal{O}(D)$  while one root has  $q \sim \mathcal{O}(1)$ . Thus the quintic reduces to

$$q^4 + 10p^2 q^2 + 24p^4 = 0 \tag{3.12}$$

at leading order, with roots  $q = \pm \sqrt{6}i p$  and  $q = \pm 2i p$ . To find whether these modes grow or decay, we consider the next order in the asymptotic expansion of  $q \sim q_0 D + q_1 + q_2 D^{-1} + \dots$ . We obtain for the roots with  $q_0 = \pm \sqrt{6}i p$ ,

$$q_1 = \frac{5}{6}(3\sigma - 2\nu - 1) \tag{3.13}$$

and for the roots with  $q_0 = \pm 2i p$ ,

$$q_1 = \frac{1}{4}(3\nu - 14\sigma). \tag{3.14}$$

The fifth root of (3.9) is  $\mathcal{O}(1)$ , and has  $q_1 = -\frac{1}{6}(\nu + 2)$ ; it is therefore always stable. Numerical solutions of (3.9) confirm that in those regions where (3.13) and (3.14) both indicate stability, i.e.

$$3\nu/14 < \sigma < \frac{1}{3}(2\nu + 1) \tag{3.15}$$

the steady solutions  $\mathbf{u}_0$  are stable for all values of  $D$ .

The results obtained in this section are summarized in fig. 4a where the  $\sigma\nu$ -plane is divided into various regions according to whether bifurcation (A) is subcritical or supercritical and whether the solution  $\mathbf{u}^0$  is stable or unstable. Region II is the only part of the plane in which the steady solutions  $\mathbf{u}^0$  remain stable for all values of  $D$ ; numerical solution of the sixth order system (1.2) confirms that for points in region II trajectories tend towards the stable limit cycle given by (2.5). In region I the roots of (3.9) that correspond to  $q \sim \pm 2i p$  are unstable; in regions III, IV and V the roots corresponding to  $q \sim \sqrt{6}i p$  are unstable. In region III bifurcation (A) is supercritical, whereas in regions IV and V the bifurcation is subcritical. In region IV the upper portion of the branch of steady solutions is stable for some values of  $D$  but in region V all steady solutions  $\mathbf{u}^0$  are unstable. The division between regions IV and V was obtained numerically but the other borders are given by simple analytical formulae.

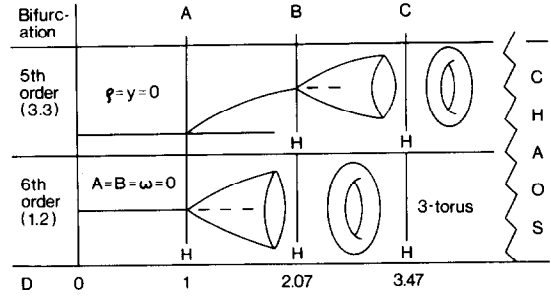
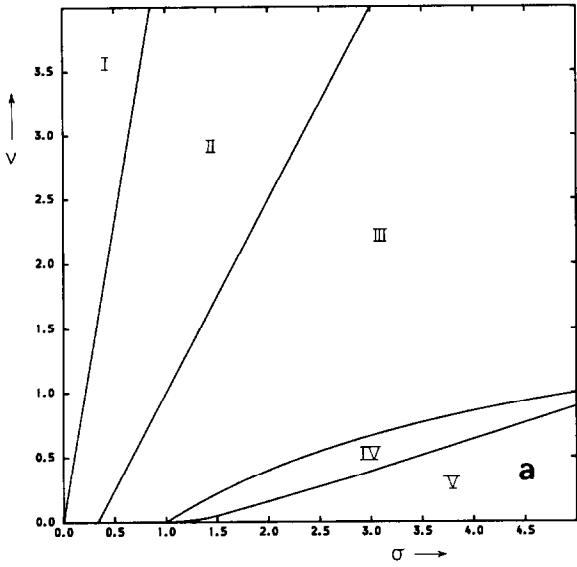


Fig. 5. Schematic bifurcation diagrams for the fifth and sixth order systems with  $\sigma = 1$ ,  $\nu = 0.5$ . Hopf bifurcations are indicated by the letter H.

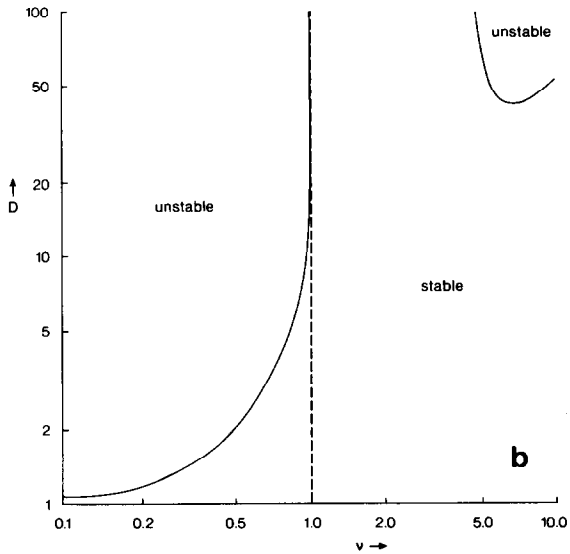


Fig. 4. a) A regime diagram for eqs. (1.1) in the  $\sigma$ - $\nu$ -plane; b) The critical value of  $D$  for the stability of the limit cycle solution of the sixth order system (1.1) as a function of  $\nu$  for  $\sigma = 1$ .

#### 4. The second bifurcation

In all parts, except region V, of the  $\sigma$ - $\nu$ -plane in fig. 4a, there are values of  $D$  for which steady, stable solutions of (3.3) exist, corresponding to stable limit cycles for the sixth order system. In

regions I, III and IV these solutions undergo a Hopf bifurcation, which we call bifurcation (B), when  $D = D_0(\nu, \sigma)$ . The bifurcation sequence for the fifth and sixth order systems is shown schematically in fig. 5. At bifurcation (B) the fixed point sheds a limit cycle, while the limit cycle of the sixth order system develops into a 2-torus. Fig. 4b shows  $D_0$  as a function of  $\nu$  for  $\sigma = 1$ . When  $\nu < 1$  (corresponding to region III of fig. 4a)  $D_0$  increases smoothly with  $\nu$ : as  $\nu \rightarrow 0$ ,  $D_0 \rightarrow 1$  and as  $\nu \rightarrow 1$ ,  $D_0 \rightarrow \infty$ . From (3.15), solutions remain stable after bifurcation (A) for  $1 < \nu < \frac{14}{3}$  (corresponding to region II) and for  $\nu > \frac{14}{3}$  (corresponding to region I) the second Hopf bifurcation occurs at a relatively high value of  $D$ . In what follows we shall mainly be concerned with behaviour in region III. Since the solution before bifurcation (B) is given in closed form, behaviour in the neighborhood of the bifurcation can be investigated analytically.

We suppose that the frequency  $s_0 = -iq$  is given by the quintic (3.9) at  $D = D_0$ . Note that this frequency will not in general be related in any simple way to the frequency  $p$  given by (2.7); in the  $A-B-\omega$  system, we expect that the motion in phase space after bifurcation (B) will lie on a 2-torus. Then for values of  $D$  close to  $D_0$  we can expand as follows:

$$\begin{aligned}
 \mathbf{u} = & \mathbf{u}^0 + \epsilon(\mathbf{u}^1 e^{i s t} + \text{c.c.}) \\
 & + \epsilon^2(D_2 \mathbf{u}_c^2 + \mathbf{u}_m^2 + \mathbf{u}_f^2 e^{2 i s t} + \text{c.c.}) + \epsilon^3 \mathbf{u}^3(t),
 \end{aligned}
 \tag{4.1}$$

where c.c. denotes the complex conjugate of the preceding term. We also expand  $D = D_0 + \epsilon^2 D_2 + \dots$ ,  $s = s_0 + \epsilon^2 s_2 + \dots$ , and  $c = c^0 + D_2 \epsilon^2 c^2$ ; for this problem  $c^2 = (0, 0, 2, 0, 0)$ . We then put these expansions into (3.6) and consider the various orders in  $\epsilon$ . At  $\mathcal{O}(1)$  we get the steady solution  $\mathbf{u}^0$ , and at  $\mathcal{O}(\epsilon)$  we get the linear solution (3.7).

We now define the linear operator  $\mathbf{L} \equiv \{l_{ij}\}$  by

$$l_{ij} = a_{ij} + b_{ikj} u_k^0 + b_{ijk} u_k^0 \quad (4.2)$$

and the corresponding adjoint operator  $\mathbf{L}^{(a)} = \{l_{ij}^{(a)}\} = \{-l_{ji}\}$ . At  $\mathcal{O}(\epsilon^2)$  we have

$$\begin{aligned} \mathbf{L} \mathbf{u}_c^2 + c^2 &= 0, \\ \mathbf{L} \mathbf{u}_m^2 + \mathbf{B}(\mathbf{u}^1, \mathbf{u}^{1*}) + \mathbf{B}(\mathbf{u}^{1*}, \mathbf{u}^1) &= 0, \\ \mathbf{L} \mathbf{u}_f^2 - 2i s u_f^2 + \mathbf{B}(\mathbf{u}^1, \mathbf{u}^1) &= 0, \end{aligned} \quad (4.3)$$

where  $\mathbf{B}(\mathbf{v}, \mathbf{w})$  denotes  $b_{ijk} v_j w_k$  and  $\mathbf{v}^*$  denotes complex conjugate of  $\mathbf{v}$ . These inhomogeneous problems can easily be solved for particular cases, though the general form of the solution in terms of  $\sigma$  and  $\nu$  is too involved to be useful.

At  $\mathcal{O}(\epsilon^3)$ , multiplying through by the adjoint solution, that is  $v^1 e^{-is_2 t}$  satisfying

$$\mathbf{L}^{(a)} v^1 + i s v^1 = 0, \quad (4.4)$$

and integrating over a cycle, we obtain

$$\begin{aligned} i s_2 \mathbf{u}^1 \cdot \mathbf{v}^1 + \mathbf{v}^1 \cdot \mathbf{B}(\mathbf{u}^{1*}, D_2 \mathbf{u}_c^2 + \mathbf{u}_m^2) \\ + \mathbf{v}^1 \cdot \mathbf{B}(D_2 \mathbf{u}_c^2 + \mathbf{u}_m^2, \mathbf{u}^{1*}) \\ + \mathbf{v}^1 \cdot \mathbf{B}(\mathbf{u}^{1*}, \mathbf{u}_f^2) + \mathbf{v}^1 \cdot \mathbf{B}(\mathbf{u}_f^2, \mathbf{u}^{1*}) &= 0. \end{aligned} \quad (4.5)$$

This equation has real and imaginary parts which determine  $s_2$  and  $D_2$ . The sign of  $D_2$  determines whether the Hopf bifurcation is subcritical or supercritical. In all the regions of fig. 4a where bifurcation (B) occurs, it is found to be supercritical. So in regions I, III and IV this second bifurcation leads to a stable limit cycle in the  $\rho$ - $x$ - $y$  system and a stable 2-torus in the  $A$ - $B$ - $\omega$  system.

In region V behaviour is more complicated. The Hopf bifurcation occurs on the lower, subcritical

branch of steady solutions  $\mathbf{u}^0$ , which already has a (real) unstable eigenvalue. Both the steady solution  $\mathbf{u}^0$  and the limit cycle shed at bifurcation (B) are therefore unstable. Numerical integration of the equations (3.3) for  $\nu = 0.5$ ,  $\sigma = 4$  suggests that solutions are chaotic for  $D \geq 5$ .

## 5. Motion on a two-torus: frequency locking and the transition to chaos

Solutions after bifurcation (B) have to be obtained numerically. We shall therefore confine our attention to behaviour in region III of fig. 4a, which is in some ways the most interesting. We discuss in detail results for  $\nu = 0.5$ ,  $\sigma = 1$ , which lies comfortably away from the boundaries of the region. (Note that  $\nu = \sigma = 1$  is not a typical case, as can be seen from fig. 4b: the solution  $\mathbf{u}^0$  is stable for all finite  $D$  but transients decay very slowly.) Then bifurcation (B) occurs at  $D = D_0 = 2.0719$ . The frequency  $p$  of the first limit cycle for the  $A$ - $B$ - $\omega$  system is then 3.0775 and the new frequency  $s_0 = 7.8186$ ; the sixth order system now has two frequencies which are typically incommensurable and we expect to find quasiperiodic motion on a 2-torus in the 6-dimensional phase space. The corresponding motion in the fifth-order system is a limit cycle.

We have obtained nonlinear solutions by solving the systems (1.2) and (3.3) numerically, using a NAGLIB routine based on a fourth order Runge-Kutta-Merson scheme with variable time-steps. Fig. 6 shows a projection onto the  $\rho^{1/2} z_r$ -plane of the limit cycle for the fifth order system (3.3) when  $D = 3.0$  (where  $x_r = \text{Re } x$  etc. and  $z_r = \rho^{1/2} x_r$ ). This periodic orbit corresponds to the 2-torus illustrated in fig. 1a. It is possible to define a Poincaré winding number  $P(D)$  for return maps like that in fig. 1b, so that  $P(D_0) = s_0/p \approx 2.54$ . In general,  $p$  varies continuously with  $D$ , passing through rational and irrational values. Because of the symmetry in this problem, there is no nonlinear coupling between  $\theta$  and the other variables (cf.

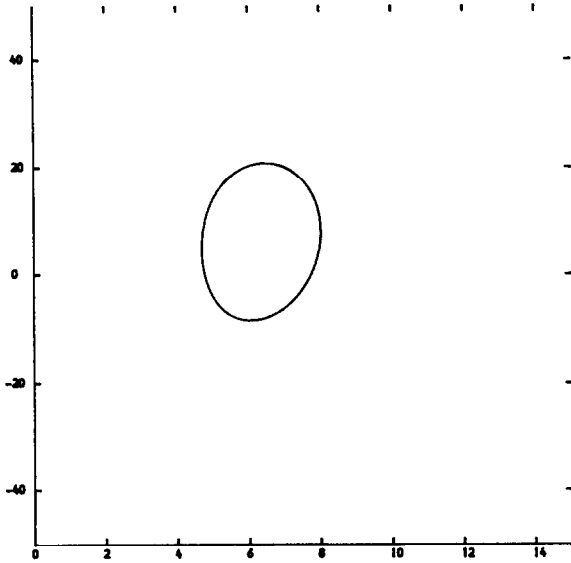


Fig. 6. A projection onto the  $\rho^{1/2}z_r$ -plane of the limit cycle solution of the fifth order system when  $D = 3.0$ ,  $\sigma = 1$ ,  $\nu = \frac{1}{2}$ .

equation (3.4)); hence  $P$  varies smoothly and there is no locking of frequencies when  $P$  is rational.

To investigate the stability of limit cycles in the  $\rho-x-y$  system we calculate eigenvalues of the linearised Poincaré return maps. These eigenvalues, the Floquet multipliers  $\lambda = e^\delta$ , are typically complex, with  $\delta = \delta_r + i\delta_i$ . The limit cycle remains stable provided all multipliers lie within the unit circle in the complex  $\lambda$ -plane ( $\delta_r < 0$ ). When  $D = D_1$  there is a further Hopf bifurcation as a pair of complex conjugate eigenvalues crosses the unit circle: we call this bifurcation (C). For  $\nu = 0.5$ ,  $\sigma = 1$  we find that  $D_1 \approx 3.4708$  and the new frequency is only 0.452, whereas the limit cycle now has a frequency of 9.268. Thus the relevant Floquet multipliers are given by  $\delta = \pm 2\pi i P_0$ , where  $P_0^{-1} \approx 20.495$ . The winding number,  $P_0$ , is fairly small and the eigenvalues cross the unit circle near the positive real axis.

Behaviour in the neighbourhood of such a bifurcation is now well understood, owing to the work of Arnol'd [10, 11, 12] (see also [13, 14]). The form of the solution depends critically on the winding number,  $P(D, \nu)$ ; in order to describe the effect of

varying  $P_0 = P(D_1, \nu)$  it is necessary to consider a two-parameter system. Let us for the moment adopt the real and imaginary parts of  $\lambda$  as parameters (rather than, say,  $D$  and  $\nu$ ). Behaviour in the neighbourhood of the bifurcation can then be followed on the sketch in fig. 7a, which shows the relevant quadrant of the complex  $\lambda$ -plane. The bifurcation occurs when  $\delta_r = 0$ , and the winding number  $P_0$  varies smoothly on the unit circle, passing through rational and irrational values, for  $\pi/2 > \delta_i > 0$ . The rational values,  $P_0 = p/q$ , where  $p, q$  are integers ( $p < q$ ), are dense but form a set of measure zero. For  $q > 4$  they give rise to weak resonances: as  $|\lambda|$  increases from unity, nonlinear interactions lead to frequency locking within a slender tongue extending from each rational value of  $P_0$ . Frequency locking with a winding number  $P = p/q$  occurs in a tongue whose width increases as  $\delta_r^{1/2(q-2)}$  immediately outside the unit circle [12]. A single parameter system, such as that obtained by increasing  $D$  for fixed  $\nu$ , passes successively through many tongues, corresponding to rational values of  $P$ . Since the tongues have finite width, the values of  $D > D_1$  for which frequency locking occurs must have a finite measure. The bifurcation pattern at each tongue resembles that shown schematically, for  $q = 5$ , in fig. 145 of ref. 12. Prior to frequency locking, trajectories are quasiperiodic and cover a torus with an irrational winding number  $P$ . A pair of periodic orbits, one stable and the other unstable, with a rational

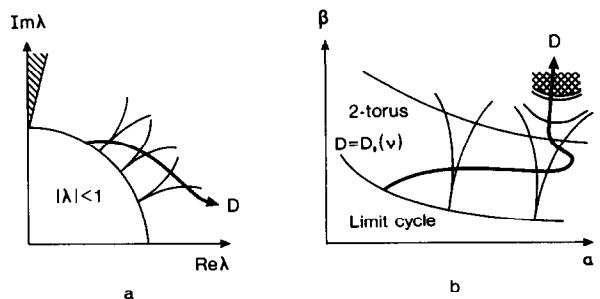


Fig. 7. a) Sketch of the tongues on which frequency locking occurs as seen in the complex  $\lambda$ -plane; b) As for a), but as seen in terms of the parameters  $\alpha(D, \nu)$  and  $\beta(D, \nu)$ .

winding number  $P = p/q$  is born at a saddle-node bifurcation and persists for a finite interval in  $D$ ; these orbits merge again and are destroyed at a second saddle-node bifurcation, where quasiperiodic motion reappears. Detailed behaviour can be understood in terms of phase portraits for the  $q$ th return map, derived from differential equations for the appropriate normal forms [12]. Before the first saddle-node bifurcation, trajectories are attracted to a circle (the cross-section of a torus) which is covered ergodically. At the bifurcation,  $q$  pairs of stable nodes and unstable saddle-points are formed on the circle. These fixed points persist until the second bifurcation, when they are destroyed and the invariant circle reappears.

As  $D$  is increased above  $D_1$ , for fixed  $\nu$ ,  $P$  varies continuously. At each rational value of  $P$  there is a pair of saddle-node bifurcations, separated by a small but finite range of  $D$  in which the frequencies are locked. Thus a graph of  $P(D)$ , if obtained with adequate resolution, would exhibit a self-similar ‘devil’s staircase’ structure. In practice, however, it is difficult to locate the tongues until  $D$  is significantly greater than  $D_1$ .

To describe the behaviour of solutions at larger values of  $|\lambda|$  it is convenient to introduce two (arbitrary but independent) parameters  $\alpha(D, \nu)$  and  $\beta(D, \nu)$ . The transition from limit cycles to 2-tori, at bifurcation (C), defines a curve in the  $\alpha\beta$ -plane, as sketched in fig. 7b.  $P$  varies continuously along this curve, with tongues extending upwards from each rational value (two of which are indicated). Increasing  $D$  for fixed  $\nu$  yields a trajectory in the  $\alpha\beta$ -plane that intersects a countable infinity of tongues. If the equations are integrated numerically it is not feasible to distinguish between quasiperiodic solutions and periodic orbits with large  $q$ . Frequency locking can only be detected in prominent tongues (i.e. those with  $q$  sufficiently small) when they have attained reasonable width (i.e. well away from bifurcation (C)). The tongues that we have found are indicated in fig. 8.

As  $D$  is increased from  $D_1$ ,  $P$  decreases from  $P_0 \approx (20.5)^{-1}$ . In order to depict numerical results

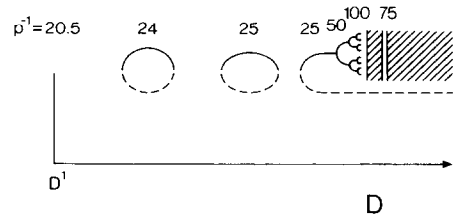


Fig. 8. Bifurcation diagram for  $D > D_1$ , i.e. after bifurcation (C).

it is preferable to use the variables

$$r = \rho^{1/2}, \quad z = rx, \tag{5.1}$$

since  $z$  remains finite as  $\rho \rightarrow 0$ . Fig. 9a shows a typical trajectory, for  $D = 3.6$ , projected onto the  $rz_r$ -plane. The corresponding return map, for the surface of section  $y_r = -2$ , is shown in fig. 9b; trajectories move round the lower curve in a clockwise sense. These results demonstrate the presence of 2-tori in the fifth-order system, corresponding to the 3-torus in fig. 2. The first example of frequency locking that we found is for  $P^{-1} = 24$ , in the interval  $3.623 \leq D \leq 3.6255$ . Fig. 10 shows a trajectory for  $D = 3.624$ , with the corresponding return map. Instead of covering the whole torus, solutions are attracted to a limit cycle wrapped round the torus with  $p = 1, q = 24$ . In order to confirm that frequency locking occurs at a saddle-node bifurcation, we used a program that finds stable or nonstable limit cycles and calculates their Floquet multipliers. At  $D \approx 3.623$  two periodic solutions come into existence, with a Floquet multiplier  $\lambda = 1$ ; thereafter, one is stable ( $|\lambda| < 1$ ), while the other is unstable (with one multiplier  $\lambda > 1$ ). Trajectories are therefore attracted to the stable solution until  $D \approx 3.6255$ , when the two solutions merge and  $\lambda = 1$ . Just above this value of  $D_1$  trajectories cover the whole torus once again.

At  $D \approx 3.687$  there is another saddle-node bifurcation and for  $3.687 \leq D \leq 3.726$  there are two periodic solutions (one stable, the other unstable) with  $q = 25$ . Note that the interval over which frequency locking occurs has increased by a factor of 16, suggesting that the tongues are swelling

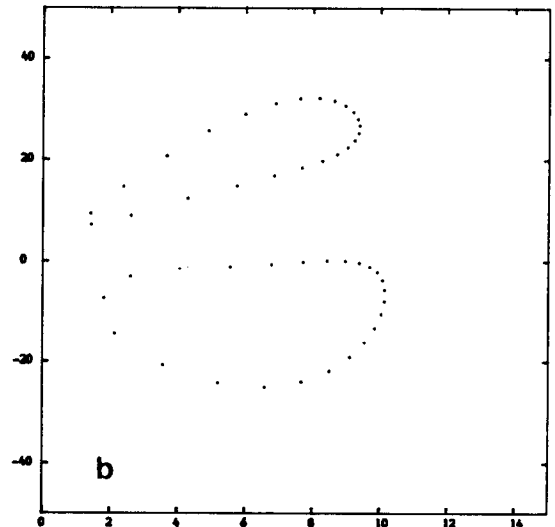
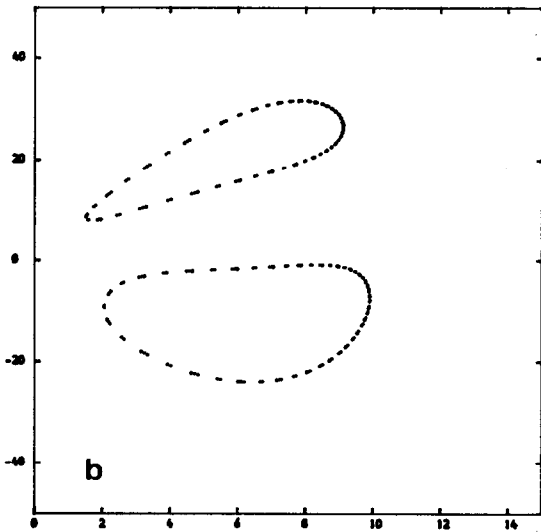
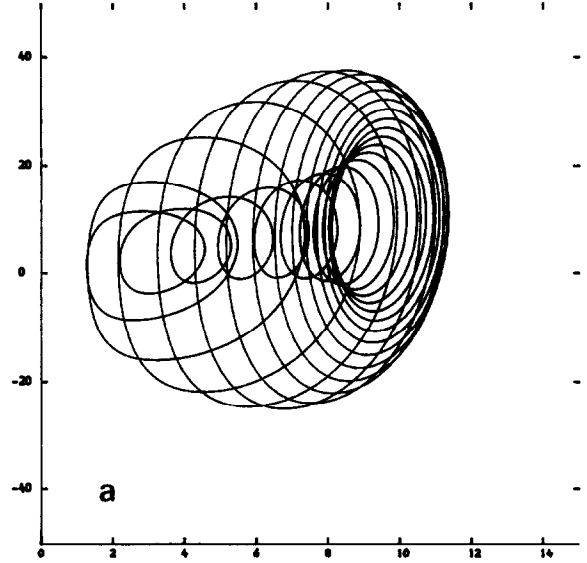
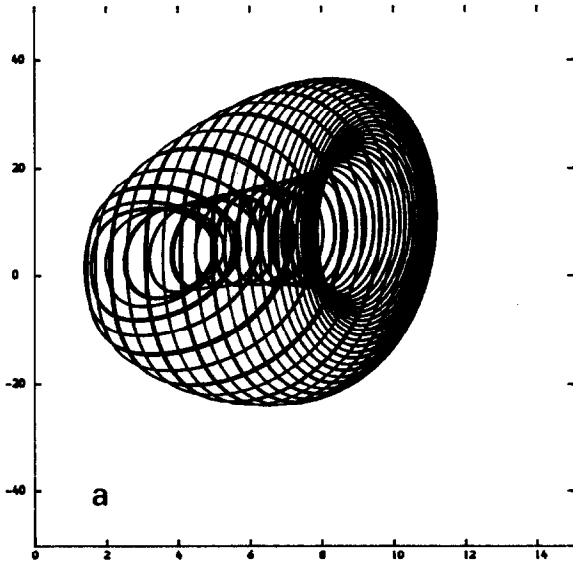


Fig. 9. a) A projection of a trajectory for the fifth order system (3.3) with  $D = 3.6$ ,  $\sigma = 1$ ,  $\nu = \frac{1}{2}$ . The projection is onto the  $rz$ -plane. If integrated for indefinite time, the whole torus would be densely covered; b) The Poincaré map for the same plane as in a) taking the section  $y_r = -2$ .

Fig. 10. a) As for 9a, but with  $D = 3.624$ . The frequency is now locked on a 24:1 ratio; b) The Poincaré map corresponding to a).

rapidly. For  $3.727 \leq q \leq 3.756$  solutions seem to be quasiperiodic but at  $D = 3.757$  there is another saddle-node bifurcation and the frequencies lock again with  $q = 25$ . The two tongues with  $P^{-1} = 24, 25$  are indicated in fig. 7b and the curve generated by increasing  $D$  is sketched; the corre-

sponding bifurcation pattern is shown in fig. 8.

So long as 2-tori exist, periodic solutions occur in tongues with rational winding numbers, separated by quasiperiodic solutions with  $P$  irrational. Eventually, the 2-tori are destroyed [15–17]. Thereafter, tongues can overlap and more than

one attractor may be present. By simultaneously varying  $\alpha$  and  $\beta$  in fig. 7b it is, in principle, possible to follow tori with any given irrational value of  $P$  until they are destroyed: a universal mechanism for the destruction of tori with  $P = \frac{1}{2}(1 + \sqrt{5})$ , the golden number, is discussed in [16] and [17], while the analogous destruction of

invariant circles in two-dimensional maps is described in [18–20]. Thus there is a curve in the  $\alpha\beta$ -plane of fig. 7b beyond which tori no longer exist. Above this curve, further bifurcations from periodic solutions may occur.

Fig. 11 shows a periodic solution for  $D = 3.8$ , which repeats itself exactly after 25 cycles. At

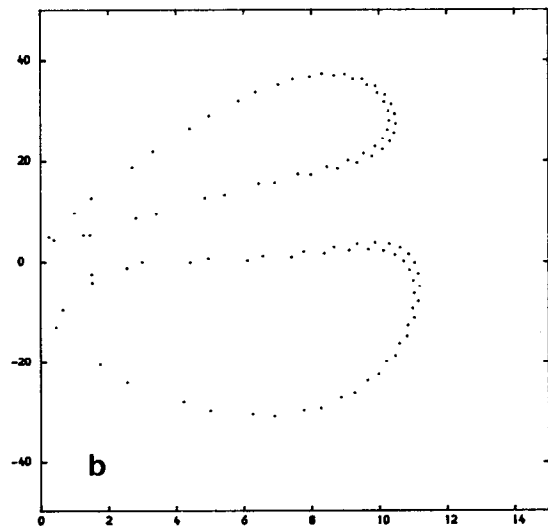
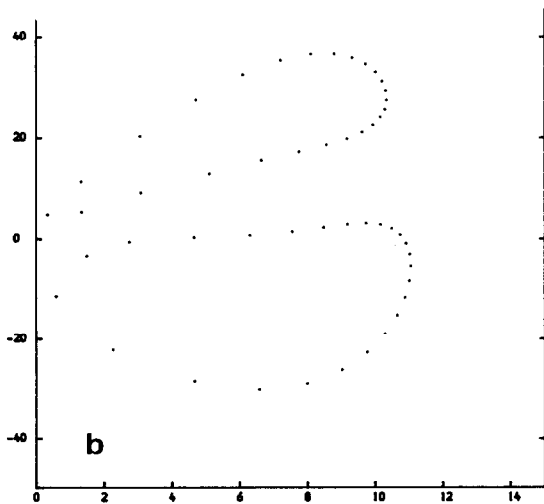
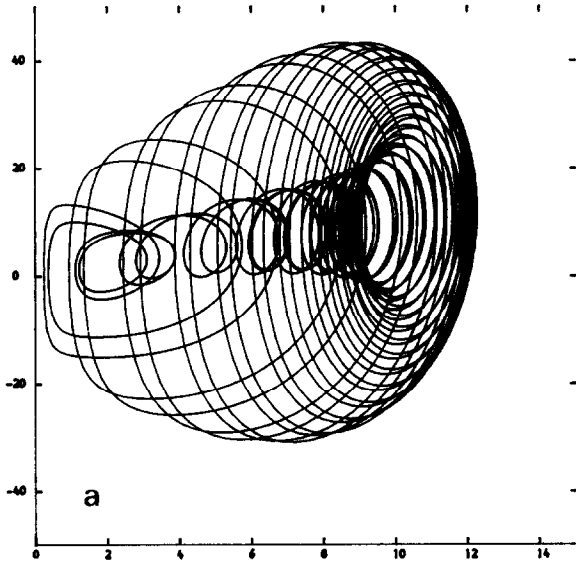
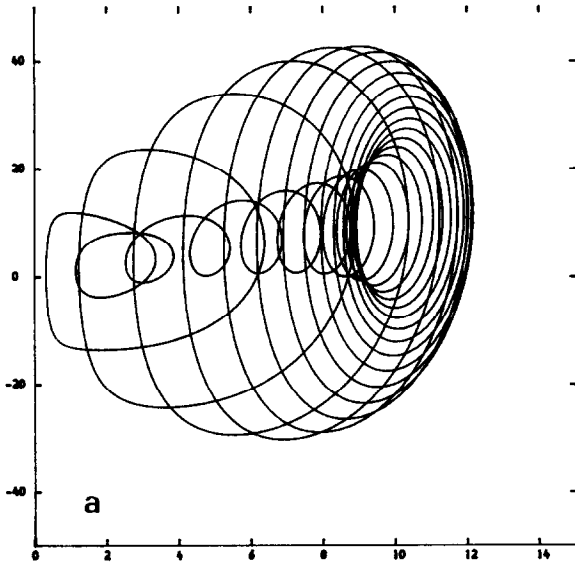


Fig. 12. a) As for 9a, but with  $D = 3.82$ . The first period-doubling bifurcation has now occurred; b) The Poincaré map corresponding to a).

Fig. 11. a) As for 9a, but with  $D = 3.80$ . The frequency is now locked on a 25:1 ratio; b) The Poincaré map corresponding to 11a.

$D = 3.806$  this solution, still locked on  $q = 25$ , becomes unstable with a Floquet multiplier passing through  $-1$ . Immediately after this bifurcation there are stable periodic solutions that repeat after  $2 \times 25$  cycles: thus the period has doubled. The new orbits cannot lie on an invariant torus and adjacent tori must have been destroyed, as indicated in fig. 7b. Fig. 12 shows a solution for  $D = 3.82$ . Comparison of the two return maps in fig. 11b and fig. 12b shows that each of the 25 points of intersection has split, giving a cycle with twice the number of points and approximately double the period. The next period-doubling bifurcation is at  $D \approx 3.8342$ . At  $D = 3.835$ , the trajectory closes on itself after  $4 \times 25 = 100$  cycles. Fig. 13b shows a detail of the return map: the pairs of points in fig. 13a, for  $D = 3.82$ , have split again and the second doubling is unmistakable. These bifurcations are shown schematically in fig. 8.

It becomes progressively harder to follow each successive period doubling in detail. At  $D = 3.836$  the period seems to be  $8 \times 25$  cycles but by  $D = 3.84$  trajectories are apparently chaotic and show no sign of settling down to periodic behaviour, even after many timesteps. Apparently there is a cascade of period-doubling bifurcations, culminating in chaos, as described by Feigenbaum [21] and others [22–24]. Similar cascades have been found in the Lorenz equations [6] and in other systems of ordinary and partial differential equations [e.g. 25, 26]. Successive period-doubling bifurcations form a sequence with an accumulation point. After the  $n$ th bifurcation we would expect to find a stable periodic solution that repeats after  $2^n \times 25$  cycles. Beyond the accumulation point solutions are typically aperiodic. Within the chaotic region there are, however, narrow windows where order is restored and stable periodic solutions reappear. Each such window has a basic period  $m$ , followed by a period-doubling cascade with periods  $m \times 2^n$  ( $n = 1, 2, \dots$ ). The first such window we have found has  $m = 74 = 3 \times 25 - 1$  and we have located this window in the narrow range  $3.901 \leq D \leq 3.903$ . At  $D = 3.901$  there is a solution that repeats after 74 cycles; the corresponding return map is shown

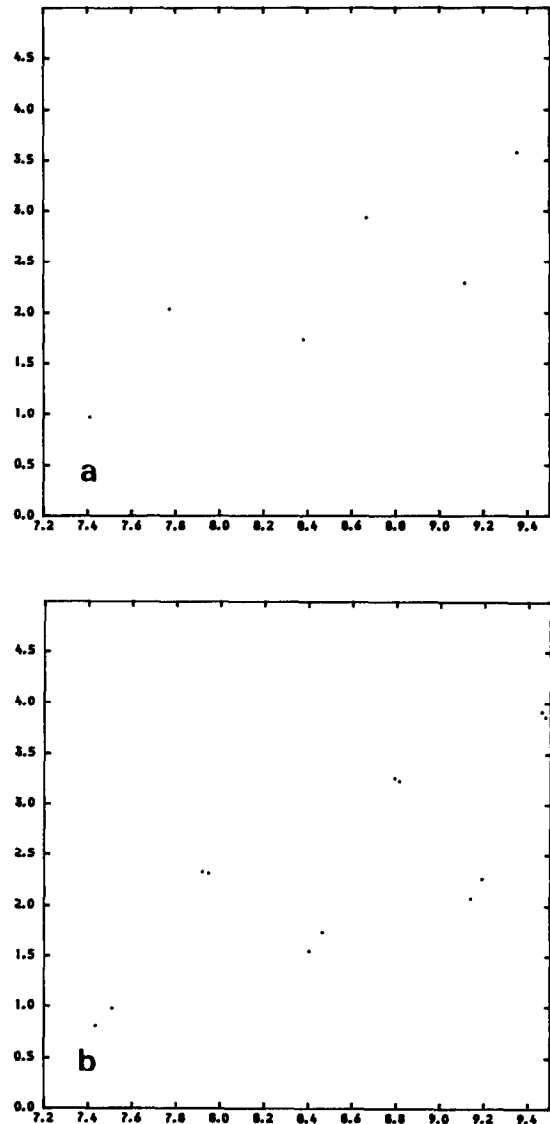


Fig. 13. a) An expanded view of 12b, at  $D = 3.82$ ; b) As for a), but with  $D = 3.835$ . The second period-doubling bifurcation has now occurred.

in fig. 14a. By  $D = 3.903$  the period has doubled and solutions repeat after  $2 \times 74 = 148$  cycles; by  $D = 3.905$  behaviour is apparently chaotic. Fig. 14b shows an example of the return map for such an aperiodic solution, at  $D = 4$ .

We have not pursued a systematic search for other periodic windows, though we have run cases up to  $D = 100$ . For all  $D \geq 4$ , solutions appeared

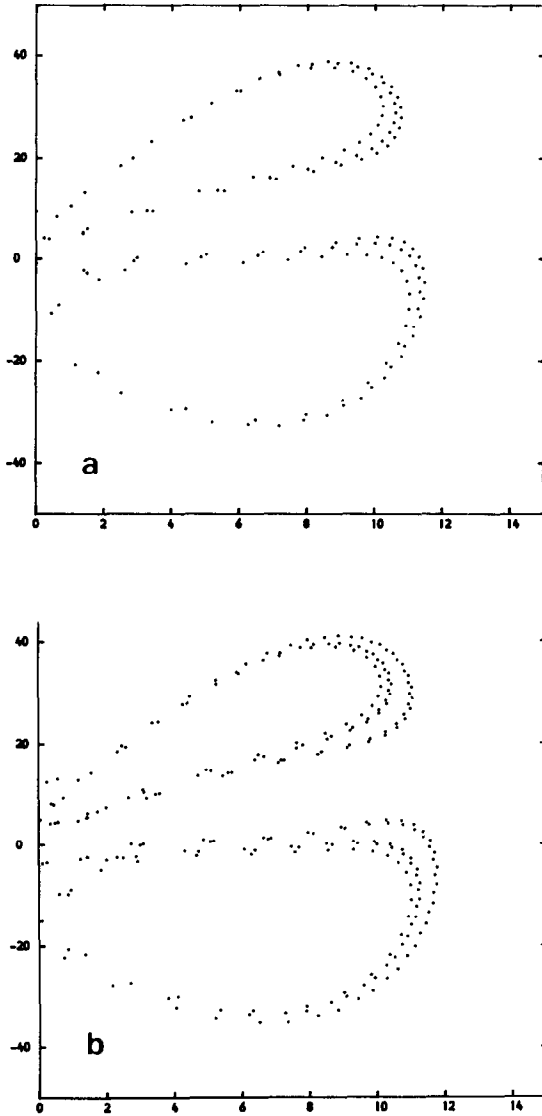


Fig. 14. a) The Poincaré map for  $D = 3.901$ , where  $D$  is in a periodic window; b) The Poincaré map for  $D = 4.0$ , where  $D$  is now in the chaotic regime.

to be chaotic. Numerical solutions for large  $D$  indicate that several different timescales are involved, though both the rapid fluctuations and the slower modulation are aperiodic. We conjecture that chaotic behaviour (interspersed with periodic windows) persists for all  $D \geq 3.84$ . It is obviously important to study solutions at large  $D$  in greater detail and their asymptotic properties in the limit

$D \rightarrow \infty$  are of considerable interest. These problems will, however, be discussed elsewhere [27].

## 6. Conclusion

Recent advances in the theory of dynamical systems have made it possible to explain the complicated behaviour exhibited by solutions of nonlinear differential equations such as (1.2). This paper demonstrates the use of a combination of analytical and numerical techniques in order to describe a succession of bifurcations that ultimately lead to chaos.

In the real Lorenz equations [5, 6], obtained by assuming that  $R$  is real in (1.3), the origin is stable for  $R < 1$ . A branch of steady solutions bifurcates from the origin at  $R = 1$ ; if  $\sigma > \nu + 1$  these solutions undergo a Hopf bifurcation. In the case most studied ( $\sigma = 10$ ,  $\nu = 8/3$ ) the Hopf bifurcation is subcritical and there is an abrupt transition to chaos; for sufficiently large  $R$ , however, only stable periodic solutions have been found. In the fifth order generalization studied by Fowler et al. [8] the origin loses stability by a Hopf bifurcation when the real part of  $R$  exceeds a critical value. The limit cycle shed at this value is stable if  $\sigma < \nu + 1$  but for  $\sigma > \nu + 1$  there is a second Hopf bifurcation, which may be subcritical or supercritical. Beyond this bifurcation, trajectories may lie on 2-tori but if the imaginary part of  $R$  is sufficiently small there is an abrupt transition to chaos, as in the real Lorenz system.

Our sixth order generalization of the Lorenz equations displays behaviour that is different. We have identified three successive Hopf bifurcations, leading to limit cycles, 2-tori, 3-tori and, eventually, chaos. From (3.15), the limit cycle is eventually unstable if  $\sigma > \frac{1}{3}(2\nu + 1)$  and chaos may appear for  $\sigma < 1$ . The second Hopf bifurcation may be subcritical and lead directly to chaos, as in the real Lorenz equations; however, we have found no evidence for a return to periodic behaviour in the range of values that we have explored.

The complex extensions of the Lorenz system all share a symmetry which makes it possible to re-

duce their order [7–9]. Transforming (1.2) to the fifth order system (3.3) facilitated our investigation: we were able to follow the branch of steady solutions and to identify Hopf bifurcations that gave birth to limit cycles and then to 2-tori. Frequency locking on the 2-tori led eventually to a periodic solution that underwent a sequence of period-doubling bifurcations that culminated in chaos. This route to chaos is not at all unusual; the only special feature of our problem is that the Feigenbaum cascade was preceded by the rather intricate periodic solution in fig. 11. We suspect that similar behaviour may occur in other systems where alternative routes to chaos have been postulated.

We have yet to establish why solutions of equations (1.2) become aperiodic. Inspection of the trajectories in figs. 8–11 shows that they approach closer to the origin as  $D$  increases. Now it follows from (3.3) that  $\rho$  remains positive for all  $D$  if  $|x|$  remains finite. We conjecture, therefore, that there is an unstable periodic solution for  $D > 3.84$ , which repeats after 25 cycles, and that this trajectory approaches the origin in  $r$ - $y$ - $z$  space asymptotically as  $D \rightarrow \infty$ . Then there is an unstable homoclinic orbit when  $D$  is infinite. For large  $D$ , the eigenvalues at the origin are  $-\frac{1}{2}(\sigma + 1) \pm \Delta$  and  $-\nu \pm 2/\Delta$  approximately, where  $\Delta^2 = \frac{1}{2}\sigma^{1/2}(\sigma + 1)D$ . Thus there are two large real eigenvalues, one positive and one negative, and a pair of complex conjugate eigenvalues with a small negative real part. Under these conditions Shil'nikov [4] proved that there will be a countable infinity of unstable periodic orbits together with an uncountable set of nonperiodic orbits [28]. Arneodo et al. [29] and Glendinning and Sparrow [30] have shown that chaos appears in the vicinity of such homoclinic bifurcations. We suggest, therefore, that the Shil'nikov mechanism is responsible for the behaviour we have found. In the neighbourhood of the origin  $|x| \approx \sqrt{2}\Delta$ , so we expect that homoclinicity cannot occur for finite  $D$ . Then chaotic behaviour should persist beyond the accumulation point of the period-doubling cascade, and the rich behaviour described in [30], which is associated

with subsidiary homoclinic orbits, cannot appear till  $D$  is infinite.

This mechanism for producing chaos from homoclinic bifurcations is robust. All that is needed is a homoclinic connection to a fixed point with eigenvalues satisfying Shil'nikov's inequality. We note that the original system (1.2) possesses a symmetry and has a trivial solution which undergoes a Hopf bifurcation and becomes increasingly unstable as the parameter  $D$  is increased. Growth is limited by nonlinear effects but the third equation has a real, negative eigenvalue at the origin. These rather general conditions ensure that Shil'nikov's inequality is satisfied but it is less easy to generate a homoclinic orbit. For instance, the limit cycles generated after bifurcation (B) do not approach the origin while they are stable; further bifurcations are needed before chaos can occur.

Similar behaviour can be expected in a variety of nonlinear systems, provided the dynamics are sufficiently complicated to allow the development of a chaotic regime. Eqs. (1.1) can be rewritten in the form

$$\begin{aligned} \frac{d^2 A}{dt^2} + 2 \frac{dA}{dt} + (1 - 2iD)A &= -iDA^* \omega, \\ \frac{d\omega}{dt} + \nu\omega &= -\frac{i}{2D}A \left( \frac{dA}{dt} + A \right). \end{aligned} \quad (6.1)$$

For  $D = 0$ , (6.1a) describes a critically damped oscillator but as  $D$  is increased damped oscillations appear and for  $D > 1$  the system is overstable, with  $A \propto \exp\{[(D^{1/2} - 1) + iD^{1/2}]t\}$ . Nonlinear saturation allows finite amplitude periodic solutions, with  $A \propto \exp i pt$ , where  $p$  satisfies (2.7) with  $\sigma = 1$ ; subsequent bifurcations follow as described above. Thus our sixth order system may be regarded as an example of a generalized nonlinear oscillator. As in the model devised by Moore and Spiegel [31, 32, 33], chaos is associated with a homoclinic bifurcation [29, 30]. The particular feature of eqs. (6.1) is that chaos is preceded by quasiperiodic behaviour and that the final Hopf bifurcation leads to oscillations with a frequency that is relatively small.

## Acknowledgements

We have benefitted from discussions with A. Bernoff, P.H. Coulet, P.A. Glendinning, J. Guckenheimer, R.S. MacKay, M.R.E. Proctor, A.M. Soward, C.T. Sparrow and H.P.F. Swinnerton-Dyer, and we are grateful for their comments and suggestions.

## References

- [1] E.N. Parker, *Cosmical magnetic fields* (Oxford, 1979).
- [2] N.O. Weiss, F. Cattaneo and C.A. Jones, *Geophys. Astrophys. Fluid Dyn.* (in press) (1984).
- [3] F. Cattaneo, C.A. Jones and N.O. Weiss, in: *Solar and stellar magnetic fields*, J.O. Stenflo, ed. (Reidel, Dordrecht, 1983).
- [4] L.P. Shil'nikov, *Dokl. Akad. Nauk SSSR* 160 (1965) 558 (*Soviet Math. Dokl.* 6 (1965) 163).
- [5] E.N. Lorenz, *J. Atmos. Sci.* 20 (1963) 130.
- [6] C.T. Sparrow, *The Lorenz Equations: Bifurcations, Chaos and Strange Attractors* (Springer, Berlin, 1982).
- [7] C.A. Jones, in: *Stellar and Planetary Magnetism*, A.M. Soward, ed. (Gordon and Breach, London, 1983), p. 159.
- [8] A.C. Fowler, J.D. Gibbon and M.J. McGuinness, *Physica* 4D (1983) 139; A.C. Fowler and M.J. McGuinness, *SIAM J. Appl. Math.* 44 (1984) 681.
- [9] M. Booty, J.D. Gibbon and A.C. Fowler, *Phys. Lett.* 87A (1982) 261.
- [10] V.I. Arnol'd, *Usp. Mat. Nauk* 27 (5) (1972) 119 (*Russ. Math. Surv.* 27 (1982) 54).
- [11] V.I. Arnol'd, *Funkts. Anal. Prilozh.* 11 (2) (1977) 1 (*Funct. Anal. Appl.* 11 (1977) 85).
- [12] V.I. Arnol'd, *Geometrical Methods in the Theory of Ordinary Differential Equations* (Springer, Berlin, 1983) (Russian version 1978).
- [13] G. Iooss and D.D. Joseph, *Elementary Stability and Bifurcation Theory* (Springer, Berlin, 1980).
- [14] O.E. Lanford, in: *Hydrodynamic Instabilities and the Transition to Turbulence*, H.L. Swinney and J.P. Gollub, eds. (Springer, Berlin, 1981), p. 7.
- [15] P.H. Coulet, C. Tresser and A. Arneodo, *Phys. Lett.* 77A (1980) 327.
- [16] D. Rand, S. Ostlund, J. Sethna and E. Siggia, *Phys. Rev. Lett.* 49 (1982) 132; S. Ostlund, D. Rand, J. Sethna and E. Siggia, *Physica* 8D (1983) 303.
- [17] M.J. Feigenbaum, L.P. Kadanoff and S.J. Shenker, *Physica* 5D (1982) 370.
- [18] S.J. Shenker, *Physica* 5D (1982) 405.
- [19] D.G. Aronson, M.A. Chory, G.R. Hall and R.P. McGehee, *Commun. Math. Phys.* 83 (1982) 303.
- [20] D. Whitley, *Bull. London Math. Soc.* 15 (1983) 177.
- [21] M.J. Feigenbaum, *J. Stat. Phys.* 19 (1978) 25.
- [22] P.H. Coulet and C. Tresser, *J. Physique* 39 (1978) C5:25; C. Tresser and P.H. Coulet, *C.R. Acad. Sci.* 207A (1978) 577.
- [23] J.P. Eckmann, *Rev. Mod. Phys.* 53 (1981) 643.
- [24] O.E. Lanford, *Ann. Rev. Fluid Mech.* 14 (1982) 347.
- [25] E. Knobloch and N.O. Weiss, *Physica* 9D (1983) 379.
- [26] D.R. Moore, J. Toomre, E. Knobloch and N.O. Weiss, *Nature* 303 (1983) 663.
- [27] C.A. Jones and H.P.F. Swinnerton-Dyer, in preparation (1985).
- [28] J. Guckenheimer, in: *Dynamical Systems and Turbulence*, Warwick 1980, D.A. Rand and L.-S. Young, eds. (Springer, Berlin, 1981), p. 55; *SIAM J. Math. Anal.* 15 (1984) 1.
- [29] A. Arneodo, P.H. Coulet, E.A. Spiegel and C. Tresser, *Physica* D, in press (1985).
- [30] P.A. Glendinning and C.T. Sparrow, *J. Stat. Phys.* 35 (1984) 645.
- [31] D.W. Moore and E.A. Spiegel, *Astrophys. J.* 143 (1966) 871.
- [32] N.H. Baker, D.W. Moore and E.A. Spiegel, *Q. J. Appl. Math.* 24 (1971) 391.
- [33] C.J. Marzec and E.A. Spiegel, *SIAM J. Appl. Math.* 38 (1980) 403.